FORWARD LINK SMART ANTENNAS AND POWER CONTROL FOR IS-136: CAPACITY INCREASE

Jack H. Winters, Carol C. Martin, and Nelson R. Sollenberger

AT&T Labs-Research
100 Schulz Drive
Red Bank, NJ 07701-7033

ABSTRACT

In this paper we study the increase in capacity using fixed-beam smart antennas and power control on the forward link in IS-136, comparing the performance with a continuous downlink, as required in IS-136, to that with a discontinuous downlink. With a continuous downlink, our beamforming technique results in a 3 and 9 dB higher signal-to-interference ratio (S/I) in the output signal with four beams versus one beam, without and with power control, respectively. With a discontinuous downlink, the S/I is 2 dB higher than with the continuous downlink with four beams, both with and without power control. Thus, most of the improvement of smart antennas and power control can be achieved even with the continuous downlink constraint by appropriate beamforming.

I. INTRODUCTION

Adaptive antenna arrays at the base stations have been shown to significantly increase the range and capacity of the uplink of the TDMA mobile radio system IS-136 [1,2,3]. However, for overall system improvement, we need to obtain range and capacity improvement on the forward link as well. Techniques that can be used by the base station to obtain these improvements include smart antennas, power control, and dynamic channel assignment [4,5].

However, in IS-136, use of these techniques is constrained by the requirement of a continuous downlink for all three time slots in each carrier. That is, the downlink beampattern and transmit power must remain the same for all users in each carrier. The carrier downlink beampattern and power can be optimized for the three users and adjusted at a rate perhaps as high as the Rayleigh fading rate (to adjust when users enter and leave the system), but cannot be changed between time slots without degrading the performance of the handsets (since most handsets use the information in the adjacent time slot to improve equalizer parameter tracking).

In a previous paper [6], we studied the increase in range using smart antennas and power control on the forward link in IS-136. Here we extend this study to the increase in capacity. We consider the increase with fixed-beam antennas in low angular-spread environments (In high angular spread environments, the capacity increase could be significantly lower [7]). We compare the performance with a continuous downlink to that with a discontinuous downlink. With a continuous downlink, our beamforming technique without power control results in about a 3 dB higher signal-to-interference ratio (S/I) in the output signal with four beams versus one beam. With power control, the S/I is increased by another 6 dB, although this gain is 3 dB when BER measurements in IS-136 are used for power control at high vehicle speeds. With a discontinuous downlink, the S/I is 2 dB higher than with the continuous downlink with four beams, both with and without power control, although the difference increases to 4 and 5 dB, without and with power control, respectively, if the base stations are synchronized (they are asynchronous in current systems). As before, the gain of power control is reduced by up to 3 dB when BER measurements in IS-136 are used for power control at high vehicle speeds. Thus, most of the improvement of smart antennas and power control can be achieved even with the continuous downlink constraint by appropriate beamforming. Furthermore, with a handset performance loss with a discontinuous downlink of about 4 dB, the use of a discontinuous downlink with today's handsets will not result in an overall improvement in performance even with smart antennas.

In Section 2 the S/I improvement with downlink beamforming without power control is described. The S/I improvement with power control is described in Section 3. A summary and conclusions are presented in Section 4.

II. S/I IMPROVEMENT WITHOUT POWER CONTROL

In this section, we consider and compare two techniques with downlink multibeam antennas for capacity increase as in [6]: a discontinuous downlink and a continuous downlink both without power control. We consider a fixed beam antenna with M non-overlapping beams over the coverage area. With a discontinuous downlink, for each user, one of M beams is chosen. With the continuous downlink requirement without power adjustment between the beams, only

0-7803-4984-9/98/$10.00 ©1998 IEEE.

those beams with users are turned on, with equal power in each beam. Thus, up to 3 beams can be turned on.

We will first consider the expected decrease in interference with discontinuous downlink as compared to a continuous downlink. Then we describe a Monte Carlo simulation of a cellular system used to study the capacity increase with multibeam antennas and discuss results.

With a discontinuous downlink, there could be a 3-fold decrease in interference as compared to a continuous downlink, but the reduction will be less than 3-fold for the following reasons. First, users are not always in separate beams. Second, carrier packing is used at the base stations such that there are fewer unused time slots to be turned off in the discontinuous case. Third, with asynchronous base stations (i.e., interference), two time slots can interfere with each time slot.

To study the capacity with multibeam antennas, Monte Carlo simulation of a cellular system was used. This simulation was based on a simulation program from Justin Chuang, which is an event-driven simulation using a model described in [8]. The cellular system consisted of hexagonal cells in a 7×14 grid with a frequency reuse (N) of 7 and a 6×6 grid with $N = 4$ (as in [9]). The base stations were located at the center of each cell, and the users were uniformly distributed in each cell. Shadow fading with a lognormal distribution was used, with a loss exponent of 3.7 and a standard deviation of 8 dB.

The simulation was event driven based on arrivals and departures. At each event, it was first determined whether the event was an arrival or departure. The probability that the event is a departure is given by $P = \frac{\mu nact}{\lambda(ntot - nact) + \mu nact}$ where $nact$ is the number of active users, λ is the arrival rate, μ is the service rate (the inverse of the length of calls), and $ntot$ is the total number of subscribers in the system. For our simulation, we set $\frac{\lambda}{\mu} = .2$ or 20% usage per user, e.g., an average call length of 3 minutes with a call every 15 minutes (note that our results did not vary significantly for $0.1 < \lambda/\mu < 0.4$). The total number of subscribers in the system depends on λ/μ, the number of sectors per cell (*nsector*), the number of channels available per sector (*nserver*), the number of cells in the system (*ncell*), the loading (*occ*), and the number of time slots (*nts*). Using typical cellular parameters, we considered a three sector system with 20 channels per sector, with 98 and 36 cells for $N = 7$ and 4, respectively, as described above. Note that 98 cells is comparable in size to the largest cellular system in current use. The probability of blockage due to no available channels is given by the Erlang B formula, and for this cellular system, a 2% blockage probability (which is a typical design goal) occurs at about 60% loading. Now, the total number of subscribers is given by

$$ntot = \left\lceil 1 + \frac{\mu}{\lambda} \right\rceil nserver \cdot nsector \cdot occ \cdot nts \cdot ncell \quad . (1)$$

Thus, with the above parameters, $ntot = 6 \cdot 20 \cdot 3 \cdot 0.6 \cdot 3 \cdot ncell = 648 ncell$, or 63,504 and 23,328 for $N = 7$ and 4, respectively.

Each simulation run begins with no active users. At the beginning, the events are mainly arrivals (note that the probability of departure is small when the number of active users is small). For each arrival, a random location is chosen for the user. The user then choses the base station with the strongest signal (with shadow fading), and determines the sector for that base station. For that sector, we considered two methods for channel (carrier) and time slot selection. In the first method, the user randomly chooses an empty time slot in a channel with at least one other user (for carrier packing). If no such time slot exists, then the user randomly chooses a time slot and channel among the unused channels for that sector. The second method is similar to the first except that S/I-based selection is used. That is, the user chooses the empty time slot in a used channel that has the lowest interference, or, if there are no empty time slots in used channels, the time slot in an unused channel with the lowest interference. (Note that we did not use the uplink S/I paired with the downlink S/I for channel selection. This method would have provided even better performance in the system.) We assumed here ideal knowledge of the interference level. As discussed in [6], there can be a few dB error in the estimation of the interference level, though, and the effect of this error is discussed below.

For each departure, an active user is randomly chosen to depart, and the S/I for that user is determined. Note that, with S/I-based carrier selection, the worst case S/I will occur, on average, at departure, since the best case occurs on arrival. (Results showed that, for the S/I-based carrier selection method, on average, the S/I at departure was about 1 dB lower than on arrival.) To study the steady state performance of the system, the distribution of this departure S/I is calculated after the time when the number of active users exceeds 90% of the steady state value, which is given by $occ \cdot ncell \cdot nserver \cdot nsector \cdot nts = 10584$ and 3888 for $N = 7$ and 4, respectively. The simulation was run for 19,600 and 7200 arrivals for $N = 7$ and 4, respectively, to ensure an adequate number of samples at a 10% cumulative probability distribution of S/I.

For the continuous downlink case, interference occurs among all users in a channel at a base station and all users in the same channel at other base stations. (With power control (see Section 3), the worst case S/I user in a beam is used to determine the transmit power for that beam.) For the discontinuous downlink case, both the

synchronous and asynchronous base station cases were studied. With asynchronous base stations, a user in one time slot is interfered with by two time slots. We assumed that the S/I in this case was given by the stronger of the two interferers.

For the antenna with M beams in a 120° sector, the antenna amplitude gain at angle θ for each beam is given by

$$af(\theta) = \frac{1}{M}\frac{\sin(M\psi)}{\sin(\psi)} \quad , \tag{2}$$

where

$$\psi = \frac{\pi}{2}\cos(\theta) \quad , \tag{3}$$

over the 120° sector, with a backlobe of -20 dB outside the sector.

Figure 1 shows the S/I distribution for $N = 7$ with random carrier/time slot selection. With a single beam, the continuous downlink has only about 1 dB lower S/I than the discontinuous downlink with synchronous base stations. The results for the discontinuous downlink with asynchronous base stations are halfway (in dB) between these two cases. Note that the difference between the continuous and discontinuous downlink cases for the single beam is due solely to the discontinuous downlink system turning off those time slots not in use. With a four-beam antenna, the S/I is 4 dB lower for the continuous downlink than for the discontinuous downlink with synchronous base stations at a 10% probability, but the four-beam continuous downlink has 3 dB higher S/I than the single beam system. Similar results were obtained for N=4, but with about a 3 dB lower S/I.

Results for S/I-based carrier/time slot selection are shown in Figure 2 for N=7. As compared to the results of Figure 1, the results in Figure 2 show that S/I-based carrier/time slot selection increases the S/I by about 1 dB over random carrier/time slot selection. Note that these results are for ideal knowledge of the interference level, and with interference estimation error, this S/I increase would be reduced somewhat. A 1 dB gain was also obtained for N=4.

Table 1 summarizes our results for the required S/I at 10% outage with N=7. For capacity increase, we note that the S/I will be about 3 dB less with N=4. These results show that the discontinuous downlink improves S/I by about 5 and 3 dB, for synchronous and asynchronous base stations, respectively, except for single beam, but this could be canceled by the 4 dB loss in handset performance at 2 GHz and 60 mph fading. The four-beam antenna improves the continuous downlink performance by 3 dB, and the discontinuous downlink performance by 5 and 6 dB for asynchronous and synchronous base stations, respectively.

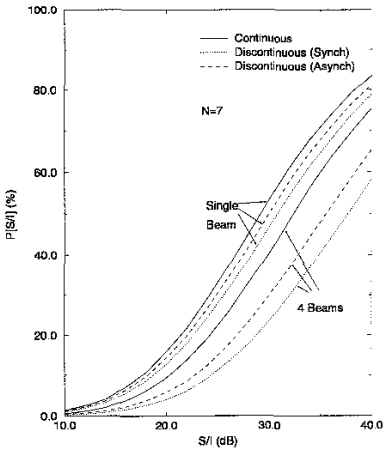

Figure 1 The S/I distribution with random carrier/time slot selection without power control for $N = 7$.

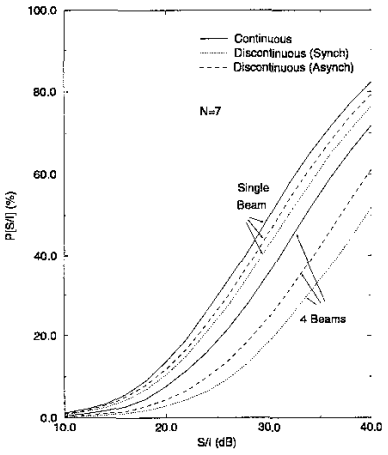

Figure 2 The S/I distribution with S/I-based carrier/time slot selection without power control for $N = 7$.

III. POWER CONTROL

With power adjustment between the beams, as shown in Figure 3, the power in each beam is adjusted so that all users meet or exceed a required S/I threshold. Specifically, with an arrival the transmit power is

TABLE 1

S/I at 10% Outage without Power Control

Power Control	Disc.	M	S/I (dB) at 10% outage N=7	
			Random	S/I-Based
No	No	1	17.6	18.4
No	No	4	20.3	21.2
No	Asynch	1	18.1	19.1
No	Asynch	4	22.8	24.1
No	Synch	1	18.6	19.7
No	Synch	4	24.4	26.3

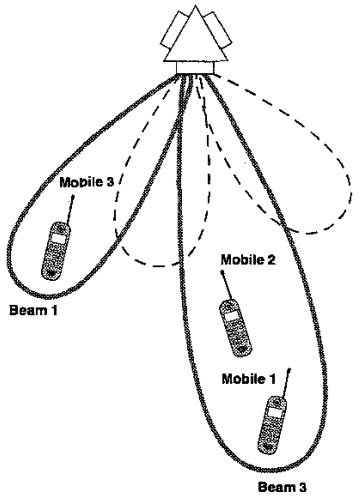

Figure 3 Downlink with fixed beams and power control.

initially set using square-root power control, i.e., the transmit power is adjusted by the square root of the propagation loss of the user. Note that this is the optimum power control strategy when a single strong interferer is present [10]. The signal-to-interference power ratio (S/I) is then determined for this user and all users that interfere with this user. If the S/I for a user is above a threshold, the transmit power for the user is decreased by 1 dB - otherwise the transmit power is increased by 1 dB, with the constraint of a maximum dynamic range of 20 dB in transmit power. This process is repeated 20 times to reach a steady state. Note that with this 1 dB adjustment the S/I can vary by up to 2 dB at each iteration. Therefore, the threshold was set to 2 dB above the required S/I to ensure that the required S/I was exceeded.

Figure 4 shows the S/I distribution with ideal power control for $N = 7$, with random carrier/time slot selection for a threshold of 22 and 26 dB with M=1 and 4, respectively. Power control is seen to greatly reduce the probability of S/I below 20 and 24 dB for M=1 and 4, respectively.

To compare the results to those without power control, we studied the S/I at 10% outage, as in Table 1. (Note that random carrier selection was used with power control in our simulation.) With power control, for each case we adjusted the threshold until the probability that the S/I was more than 2 dB below threshold was equal to 10%. Table 2 shows the S/I at 10% outage with ideal power control. Ideal power control is seen to improve performance by about 4 to 6 dB with either continuous or discontinuous downlinks.

From Tables 1 and 2, note also that for the discontinuous downlink with synchronous base stations, the increase in S/I due to power control is the same for 1 and 4 beams (6.5 dB). However, with the continuous downlink, the increase in S/I due to power control is 2.2 dB higher for 4 beams versus 1 beam (5.8 versus 3.6 dB). Thus, for the continuous downlink the combination of smart antennas and power control provides greater gain than the sum of the gains of each technique by itself.

We next studied the effect of error in the S/I estimation. For S/I estimation, we consider the use of the quantized BER measurement. We used BER measurement results [6, Figure 3] from a field trial where the vehicle speed was about 45 mph. As can be seen from [6, Figure 3], using the BER measurements, the received signal power estimation error (in dB) has an approximately Gaussian distribution with a standard deviation of 3 dB. Now, for S/I estimation, the BER depends on the difference in desired and interfering signal powers. As seen from [6, Figure 3], the received signal power error after one second also has an approximately Gaussian distribution with a standard deviation of about 1.6 dB. Thus, we would expect the distribution of S/I estimation error to also be Gaussian with a standard deviation of about 3.5 dB ($\sqrt{3^2+1.6^2}$) with a single (dominant) interferer. Note that the standard deviation would be somewhat less with multiple interferers, and less if either the desired or interfering mobiles were not moving rapidly.

Now, with BER-based power control, the S/I estimation is made once per second. Thus, with power control adjustment over a 20 second interval, the variation in the S/I over this interval must also be considered. Figure 5 shows the standard deviation of the received signal power difference with delays up to 20 seconds from our field trial data. If the received

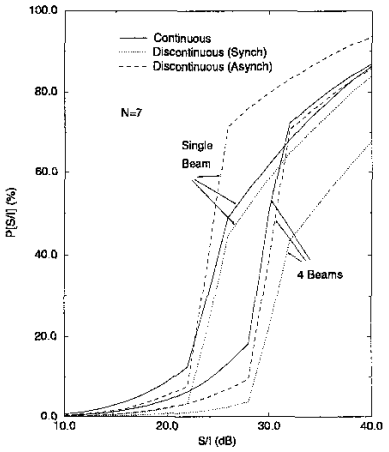

Figure 4 The S/I distribution with ideal power control for $N = 7$.

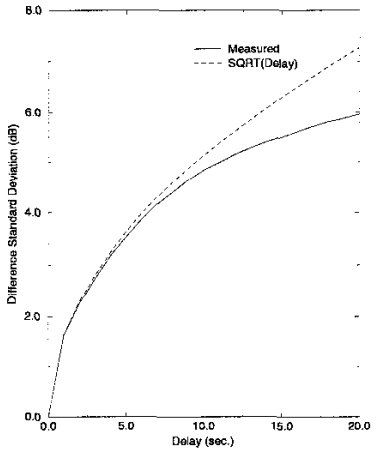

Figure 5 The standard deviation of the received signal power difference with delay.

TABLE 2

S/I at 10% Outage with Ideal Power Control

Power Control	Disc.	M	S/I (dB) at 10% outage N=7
Ideal	No	1	21.2
Ideal	No	4	26.1
Ideal	Asynch	1	22.5
Ideal	Asynch	4	28.1
Ideal	Synch	1	25.1
Ideal	Synch	4	30.9

power changed independently from one second to the next (a random walk), then this standard deviation would increase with the square root of the time difference, as shown by the dashed curve in Figure 5. However, the signal power typically has a lognormal distribution, with a mean that does not vary significantly over 20 seconds (since it is distance dependent), and a standard deviation of about 8 dB. Thus, the value of the standard deviation with time difference will saturate at this standard deviation, as shown in Figure 5. Therefore, in our simulation program we model the change in S/I with time as a filtered Gaussian process with the filter coefficients set to give the standard deviation increase shown in Figure 5. (Since the S/I is the ratio of two filtered Gaussian processes, the filter coefficients for S/I are actually given by the convolution of the filter coefficients of Figure 5, but this should not significantly affect our results.) Specifically, the ith filter coefficient, $\alpha(i)$ is given by

$$\alpha^2(i) = \frac{\sigma^2(i)}{\sigma_s^2} - \sum_{j=1}^{i-1}\alpha^2(j) \quad , \tag{4}$$

where $\sigma(i)$ is the standard deviation with an i second delay (from Figure 5) and σ_s is the standard deviation of the received signal power difference with a one second delay (1.6 dB from [6]).

Therefore, combining the BER-based estimation error and S/I variation, the S/I at the ith iteration of the power control method is given by

$$S/I(i) = S/I(0) + v(i) \tag{5}$$

where

$$v(i) = y(i) + \sum_{j=1}^{i-1} y(j)\alpha(i-j+1)\sqrt{\frac{2\sigma_s^2}{\sigma_b^2 + \sigma_s^2}} \quad , \tag{6}$$

$y(i)$ is a Gaussian random variable with zero mean and standard deviation σ_b, and σ_b is the standard deviation of the difference between the received signal power and the estimated power based on BER with a one second

delay (3 dB from [6]). Note that the term $\sqrt{\frac{2\sigma_s^2}{\sigma_b^2 + \sigma_s^2}}$ adjusts for the fact that the BER-based estimation error does not affect the S/I variation with time.

Because of the variation in signal power with time using this model, the base station with the smallest propagation loss can change over the 20-second interval for power control adjustment. In practice, a handoff could occur, but to simplify our simulation program, we did not incorporate handoffs. Thus, the variation in signal power with time causes the system performance to degrade over the 20-second interval without power control. Therefore, for our results we define the gain due to power control as the increase in S/I at the end of the 20-second interval over that without power control for a given σ_s and σ_b.

Table 3 shows the S/I at 10% outage with BER-based power control for N=7. For these results, the threshold was adjusted in each case to maximize the S/I at 10% outage, and the optimum threshold was typically about 4 dB above the S/I shown. These results show that BER-based power control provides about half (in dB) of the gain of ideal power control in most cases. However, these results are for a vehicle speed of about 45 mph, and at lower speeds the effect of the reporting delay is less, which results in a greater power control gain.

IV. CONCLUSIONS

In this paper we studied the increase in capacity using smart antennas and power control on the forward link in IS-136. We considered the increase with fixed-beam antennas in low angular-spread environments, transmit power control, and interference-based time slot/carrier selection. With a continuous downlink, our beamforming technique provides about a 3 and 9 dB higher signal-to-interference ratio (S/I) in the output signal with four beams versus one beam, without and with power control, respectively. However, the increase with power control is reduced by about 2 dB when BER-based power control is used at high vehicle speeds. With a discontinuous downlink, the S/I is 2 to 3 dB higher than with the continuous downlink with four beams, although the difference increases up to 5 dB if the base stations are synchronized. Thus, most of the improvement of smart antennas and power control can be achieved even with the continuous downlink constraint by appropriate beamforming. Furthermore, with a handset performance loss with a discontinuous downlink of about 4 dB, the use of a discontinuous downlink with today's handsets will not result in an overall improvement in performance even with smart antennas.

TABLE 3

Gain in S/I at 10% Outage with BER-Based versus Ideal Power Control

Disc.	M	Power control gain (dB) (N=7)	
		Ideal	BER-Based
No	1	3.6	2.1
No	4	5.8	3.3
Asynch	1	4.4	4.0
Asynch	4	5.3	4.2
Synch	1	6.5	3.8
Synch	4	6.5	3.3

V. ACKNOWLEDGEMENT

We gratefully acknowledge useful discussions with Justin Chuang and Jim Whitehead.

REFERENCES

[1] J. H. Winters, "Signal acquisition and tracking with adaptive arrays in the digital mobile radio system IS-54 with flat fading," *IEEE Trans. on Vehicular Technology*, November 1993.

[2] R. L. Cupo, G. D. Golden, C. C. Martin, K. L. Sherman, N. R. Sollenberger, J. H. Winters, and P. W. Wolniansky, "A four-element adaptive antenna array for IS-136 PCS base stations," *Proc. of VTC'97*, May 4-7, 1997, pp. 1577-1581.

[3] R. L. Cupo, J. Curlo, G. D. Golden, W. Kaminski, C. C. Martin, D. J. Mastriani, E. Rosenbergh, P. D. Sharpe, K. L. Sherman, N. R. Sollenberger, J. H. Winters, P. W. Wolniansky and T. Zhuang, "Adaptive antenna applique field test," *Fourth Annual Workshop on Smart Antennas in Wireless Communications*, Stanford University, July 24-25, 1997, submitted to *IEEE Trans. on Vehicular Technology*.

[4] G. V. Tsoulos, M. A. Beach, and S. C. Swales, "Sensitivity analysis of capacity enhancement with adaptive multibeam antennas for DCS1800," *Electronics Letters*, Sept. 12, 1996, pp. 1745-6.

[5] Y. Li, M. J. Feuerstein, and D. O. Reudink, "Performance evaluation of a cellular base station multibeam antenna," *IEEE Transactions on Vehicular Technology*, Feb. 1997, pp. 1-9.

[6] J. H. Winters, C. C. Martin, and N. R. Sollenberger, "Forward Link Smart Antennas and Power Control for IS-136," *Proc. of the IEEE Vehicular Technology Conference*, Ottawa, Canada, May 19-21, 1998.

[7] J. H. Winters and M. J. Gans, "The Range Increase

of Adaptive versus Phased Arrays in Mobile Radio Systems," *Proc. of Asilomar Conference on Systems, Signals, and Computers*, Pacific Grove, CA, 1994.

[8] R. C. Bernhardt, "Time-slot management in digital portable radio systems," *IEEE Transactions on Vehicular Technology*, Feb. 1991.

[9] J. F. Whitehead, "Performance and capacity of distributed dynamic channel assignment and power control in shadow fading," *Proc. IEEE International Conference on Communications*, Geneva, Switzerland, May 1993, pp. 910-914.

[10] Z. J. Haas, J. H. Winters, and D. S. Johnson, "Simulation results of the capacity of cellular systems," *IEEE Transactions on Vehicular Technology*, Nov. 1997, pp. 805-817.